

Electron-ion recombination in low temperature hydrogen/deuterium plasma[★]

Juraj Glosik^{1,*}, Petr Dohnal¹, Ábel Kálosi¹, Lucie D. Augustovičová², Dmytro Shapko¹, Štěpán Roučka¹, and Radek Plašil¹

¹ Department of Surface and Plasma Science, Faculty of Mathematics and Physics, Charles University, 18000 Prague, Czech Republic

² Department of Chemical Physics and Optics, Faculty of Mathematics and Physics, Charles University, 12116 Prague, Czech Republic

Received: 28 June 2017 / Received in final form: 16 October 2017 / Accepted: 21 November 2017

Abstract. The stationary afterglow with cavity ring down spectrometer (SA-CRDS) was used to study the recombination of H_3^+ , H_2D^+ , HD_2^+ and D_3^+ ions with electrons in low temperature (77–300 K) plasmas in He/Ar/ H_2/D_2 gas mixtures. By measuring effective recombination rate coefficients (α_{eff}) in plasma with mixtures of ions and their dependences on temperature and partial densities of He, H_2 and D_2 , $\alpha_{\text{eff}}(T, [\text{He}], [\text{H}_2], [\text{D}_2])$, we determined binary (α_{binH_3} , $\alpha_{\text{binH}_2\text{D}}$, α_{binHD_2} , α_{binD_3}) and ternary (K_{H_3} , $K_{\text{H}_2\text{D}}$, K_{HD_2} , K_{D_3}) recombination rate coefficients for H_3^+ , H_2D^+ , HD_2^+ and D_3^+ ions. For all four ions we observed very efficient He assisted ternary recombination which is comparable with binary recombination already at $[\text{He}] = 1 \times 10^{17} \text{ cm}^{-3}$. The removal of excited particles in afterglow plasma was monitored to obtain the plasma thermalisation rate at given experimental conditions. The inferred deexcitation rates for reaction of helium metastable atoms with D_2 are $k_{\text{D}_2}(300 \text{ K}) = (2.1 \pm 0.3) \times 10^{-10} \text{ cm}^3 \text{ s}^{-1}$ and $k_{\text{D}_2}(140 \text{ K}) = (1.3 \pm 0.3) \times 10^{-10} \text{ cm}^3 \text{ s}^{-1}$.

1 Introduction

The dissociative recombination of H_3^+ cation and its deuterated isotopologues H_2D^+ , HD_2^+ and D_3^+ has been investigated for nearly six decades (see e.g. Refs. [1,2]). This extensive research is motivated by fundamental character of processes of recombination of these ions. Further motivation is in astrophysics, plasma physics and in technological applications of hydrogen and deuterium plasmas. Ions H_3^+ , H_2D^+ and HD_2^+ have been detected many times in the interstellar medium [3,4]. All four isotopologues of H_3^+ are included in the current models of interstellar chemistry of molecular clouds [5–7]. The degree of deuteration of ions in H_2/D_2 buffered plasmas depends on physical conditions such as the $[\text{D}_2]/[\text{H}_2]$ ratio, temperature and overall pressure. Essential are also the rates of formation and destruction of these ions in actual plasmatic environments.

Having in mind low temperature plasmas and their technological applications, the present study focuses on binary and neutral assisted ternary electron-ion recombination processes [8–10] in plasmas containing both hydrogen and deuterium. The employed experimental technique (discussed in the next section) enables in situ probing of

number densities of all four isotopologues of H_3^+ in afterglow plasma. A particular attention was given to the plasma thermalisation by monitoring the presence and rate of removal of excited particles in the afterglow and the kinetic and the rotational temperatures of the recombining ions.

2 Characterisation of afterglow plasma in He/Ar/ H_2/D_2 gas mixture

For measurements of recombination rate coefficients we use a standard stationary afterglow (SA) experiment with cavity ring down absorption spectrometer (for details see [8] and references therein). In afterglow experiments time evolutions of electron and ion number densities are monitored during the decay of the recombination dominated afterglow plasma. In the present experiments a plasma is formed by microwave discharge in a He/Ar/ H_2/D_2 gas mixture with typical number densities of $5 \times 10^{17}/10^{14}/10^{14}/10^{14} \text{ cm}^{-3}$, respectively. The flows of helium buffer gas and reactants are monitored by MKS mass flow meters and controllers and the pressure in the discharge tube is measured by MKS Baratron Type 622 and by PTU-F-AC3-32AH piezo pressure transducer enabling us to determine the corresponding partial number densities. If the desired reactant flow is lower than achievable by the flow controller, we create mixture of the reactant with helium in a reservoir equipped with absolute MKS Baratron Type 122A. In such way number densities down to 10^{11} cm^{-3} are achievable. During the discharge and in the very early afterglow the plasma contains

[★] Contribution to the topical issue “Plasma Sources and Plasma Processes (PSPP)”, edited by Luis Lemos Alves, Thierry Belmonte and Tiberiu Minea.

* e-mail: juraj.glosik@mff.cuni.cz

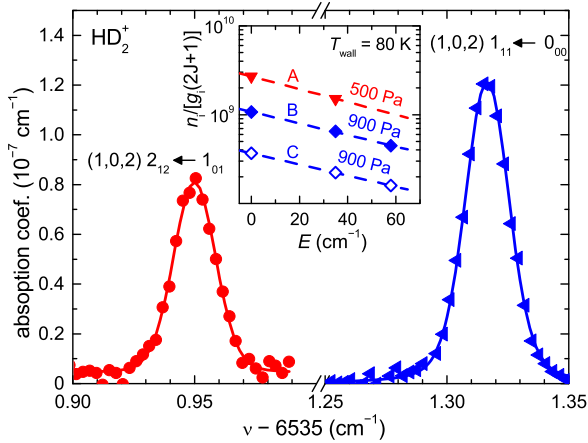


Fig. 1. The absorption line profiles obtained for HD_2^+ ions at $T_{\text{wall}} = 80$ K in a mixture of He/Ar/ H_2 / D_2 with $[\text{He}] = 4.0 \times 10^{17} \text{ cm}^{-3}$, $[\text{Ar}] = 2.1 \times 10^{14} \text{ cm}^{-3}$, $[\text{H}_2] = [\text{D}_2] = 9 \times 10^{13} \text{ cm}^{-3}$. The particular transitions are shown at the top of each plot and denoted by corresponding vibrational (v_1, v_2, v_3) and rotational $J_{K_a K_c}$ quantum numbers, for details see reference [13]. The insert shows Boltzmann plots obtained for HD_2^+ ($T_{\text{wall}} = 80$ K) at two different pressures of He buffer gas. The filled symbols (A and B) denote values obtained in the discharge while the values indicated by open symbols (C) were measured 100 μs after switching off the discharge. The obtained rotational temperatures are: $T_{\text{rotA}} = (87 \pm 10)$ K, $T_{\text{rotB}} = (96 \pm 10)$ K and $T_{\text{rotC}} = (98 \pm 15)$ K while the kinetic temperature evaluated from the Doppler broadening of the plotted absorption lines is $T_{\text{kin}} = (96 \pm 10)$ K.

electrons, ions (H_3^+ , H_2D^+ , HD_2^+ and D_3^+), and some highly excited particles. The temperature of the electrons (T_e) during the discharge is on the order of ~ 2 eV. After switching off the discharge (microwaves) electrons are cooled in collisions with He, assuming that they are not heated in collisions with highly excited metastable Ar or He particles [11]. The electron temperature in the afterglow can be determined by monitoring losses of charged particles due to the ambipolar diffusion [12].

The determination of plasma parameters during the active discharge and during the afterglow is obviously a first step in the experiment. Important parameters are those that characterise thermalisation of afterglow plasmas. For example the equality within the error of measurement between the kinetic (T_{kin}) and the rotational (T_{rot}) temperature of ions, the temperature of the buffer gas (T_{He}), and the wall temperature of the discharge tube (T_{wall}) needs to be experimentally verified. By measuring the corresponding absorption line profiles T_{rot} , T_{kin} and ion densities can be determined for all four ions. Examples of absorption lines profiles measured for HD_2^+ ions at $T_{\text{wall}} = 80$ K are shown in Figure 1. From the obtained Boltzmann plots (examples are shown in the insert) T_{rot} are evaluated during the discharge and during the early afterglow. The kinetic temperature is evaluated from the Doppler broadening of the measured absorption lines. As the T_{kin} and T_{rot} of H_2D^+ and HD_2^+ ions are very close to each other and to the T_{wall} and the same also applies for H_3^+ and D_3^+ ions [8,9], in the following text we will use only single temperature T with numerical value of T_{wall} if not stated otherwise.

Table 1. Measured transitions (ν_{exp}) belonging to the (1–0) vibrational band of the $\text{He}_2 \text{b}^3\Pi_g - \text{a}^3\Sigma_u^+$ system compared to the calculated values (ν_{calc}). For details on the calculations see reference [11]. The estimated error of the measurement is $5 \times 10^{-4} \text{ cm}^{-1}$. The calculated Einstein coefficients of spontaneous emission A are also listed. The transitions are labeled with the corresponding quantum numbers $\Delta J_{F'F''}(N'')$, where $F=1$ for $J=N+1$, $F=2$ for $J=N$, and $F=3$ for $J=N-1$ and the prime and double prime denote the upper and lower state, respectively.

Transition	$\nu_{\text{exp}} (\text{cm}^{-1})$	$\nu_{\text{calc}} (\text{cm}^{-1})$	$A (10^4 \text{ s}^{-1})$
$\text{P}_{22}(9)$	6296.0566	6296.0538	3.9
$\text{P}_{11}(9)$	6296.1462	6296.1438	4.8
$\text{P}_{33}(9)$	6296.2220	6296.2199	2.9
$\text{R}_{11}(1)$	6494.2730	6494.2729	3.3
$\text{R}_{22}(21)$	6533.6633	6533.6946	7.4
$\text{R}_{11}(21)$	6533.7675	6533.7651	6.8
$\text{R}_{33}(21)$	6533.8086	6533.8085	8.1

To confirm thermalisation of electrons within the very early afterglow we have monitored the time decay of the densities of the $\text{a}^3\Sigma_u^+$ ($N=9, J=10$) excited state of He_2 and the $3s^23p^5(^2\text{P}_{1/2}^o)3d^2[3/2]^o, J=2$ excited state of argon that indirectly hint on the presence of helium metastable atoms [11]. The corresponding transitions are listed in Table 1 and in reference [11]. The present measurements were carried out in pure He, He/Ar, He/Ar/ H_2 and in He/Ar/ H_2 / D_2 mixtures in order to characterise the time constant τ for deexcitation in collisions with Ar, H_2 and D_2 . The examples of measured dependences of inverse time constants ($1/\tau$) of the decays of the density of excited (He_2)* and (Ar)* on $[\text{D}_2]$ and $[\text{H}_2]$ are plotted in Figure 2. The slope of the linear fit to the data in Figure 2 gives effective rate coefficients of de-excitation for metastable helium atoms in collisions with D_2 or H_2 (see discussion and explanation in Ref. [11]): $k_{\text{D}_2}(300 \text{ K}) = (2.1 \pm 0.3) \times 10^{-10} \text{ cm}^3 \text{ s}^{-1}$ and $k_{\text{D}_2}(140 \text{ K}) = (1.3 \pm 0.3) \times 10^{-10} \text{ cm}^3 \text{ s}^{-1}$. These values are approximately 30% lower than the corresponding rates obtained for H_2 reactant gas [11]. Under conditions for which the data plotted in Figure 1 were measured and which are typical for current experiments, the plasma (ions and electrons) is thermalised in time shorter than 100 μs .

3 Electron–ion recombination in He/Ar/ H_2 / D_2 gas mixtures

In this section we will summarise the complications connected with evaluation of recombination rate coefficients in plasmas containing both H_2 and D_2 . The ions H_3^+ , H_2D^+ , HD_2^+ and D_3^+ formed in discharge in He/Ar/ H_2 / D_2 gas mixtures are during the decay of an afterglow plasma removed by recombination with electrons and by ambipolar diffusion. In description of such plasmas we have to consider several recombination processes, e.g. for H_2D^+ ions:

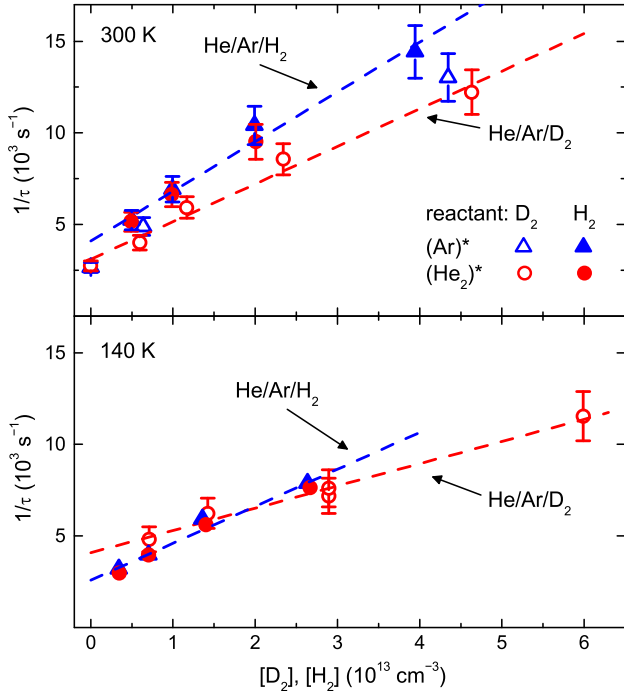
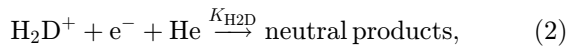
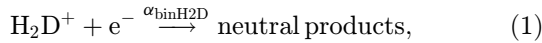


Fig. 2. Dependences of the reciprocal time constants of exponential decays of $(He_2)^*$ and $(Ar)^*$ number densities on $[D_2]$ measured in the afterglow at 300 K (upper panel) and at 140 K (lower panel). The values obtained in a He/Ar/D₂ gas mixture (open circles for $(He_2)^*$ and open triangles for $(Ar)^*$) are compared to those previously measured in a He/Ar/H₂ gas mixture (filled circles and filled triangles for $(He_2)^*$ and $(Ar)^*$, respectively) [11]. In the present experiment the helium buffer gas pressure was 900 Pa and $[Ar]=5 \times 10^{12} \text{ cm}^{-3}$ at 300 K and $[Ar]=7 \times 10^{12} \text{ cm}^{-3}$ at 140 K. The dashed lines are linear fits to the data.



where α_{binH2D} and K_{H2D} are binary and ternary (He assisted) recombination rate coefficients. Ions H_3^+ , HD_2^+ and D_3^+ recombine similarly with rate coefficients α_{binH3} , α_{binHD2} , α_{binD3} , K_{H3} , K_{HD2} and K_{D3} . In agreement with present results and results of previous experimental studies, we assume that binary and three-body recombination processes add linearly, i.e. that an “effective” rate coefficient can be defined as $\alpha_{\text{effion}} = \alpha_{\text{binion}} + K_{\text{ion}}[\text{He}]$. The linear combination is known to become invalid at high He densities due to saturation (high pressure limit) [14]. For recombination dominated quasineutral afterglow plasma the balance equation for electron density is:

$$\frac{\partial n_e}{\partial t} = -(\alpha_{\text{effH3}}[H_3^+] + \alpha_{\text{effHD2}}[H_2D^+] + \alpha_{\text{effHD2}}[HD_2^+] + \alpha_{\text{effD3}}[D_3^+])n_e - n_e/\tau_{\text{RD}}. \quad (3)$$

The term n_e/τ_{RD} describes losses due to ambipolar diffusion and due to possible conversion to other ion species (for more detailed description of kinetics of processes see Refs. [14–16]). By using the fractions f_{H3} , f_{H2D} , f_{HD2} and f_{D3} for all ions ($f_{\text{ionX}} = [X^+]/n_e$) instead of the ion number

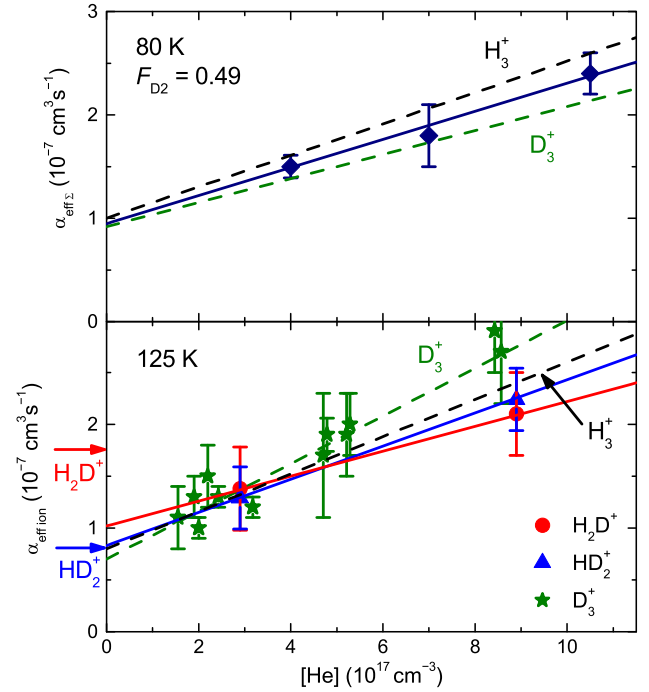


Fig. 3. The dependence of $\alpha_{\text{eff}\Sigma}$ on $[\text{He}]$ obtained at 80 K for $F_{D_2} = 0.49$. The dashed lines denoted H_3^+ and D_3^+ are linear fits to the α_{effH3} and α_{effD3} taken from reference [10]. Lower panel: The dependences of α_{effH2D} and α_{effHD2} on $[\text{He}]$ measured at 125 K. The full lines are linear fits to the data used to obtain the recombination rate coefficients α_{binH2D} , α_{binHD2} , K_{H2D} and K_{HD2} . The dashed lines denoted H_3^+ and D_3^+ are linear fits to the α_{effH3} and α_{effD3} [10]. The arrows indicate the theoretical values of α_{binH2D} and α_{binHD2} [17]. The stars denote the values measured for D_3^+ in SA-CRDS experiment (see also Ref. [8]).

densities the balance equation (3) can then be written in the simple form:

$$\frac{\partial n_e}{\partial t} = -\alpha_{\text{eff}\Sigma} n_e^2 - n_e/\tau_{\text{RD}} \quad (4)$$

where the overall effective recombination rate coefficient $\alpha_{\text{eff}\Sigma}$ is equal to the sum: $\alpha_{\text{eff}\Sigma} = \alpha_{\text{effH3}}/f_{H3} + \alpha_{\text{effHD2}}/f_{HD2} + \alpha_{\text{effH2D}}/f_{H2D} + \alpha_{\text{effD3}}/f_{D3}$. The ionic composition at constant temperature and constant $[\text{He}]$ is given by the relative densities of D₂ and H₂, which can be characterised e.g. by relative D₂ density, $F_{D_2} = [D_2]/([H_2] + [D_2])$. It is obvious that if $\alpha_{\text{eff}\Sigma}$ is measured for several ionic compositions of plasma then the values of particular effective recombination rate coefficients $\alpha_{\text{effion}}(T, [\text{He}])$ can be obtained. From the dependence of $\alpha_{\text{effion}}(T, [\text{He}])$ on $[\text{He}]$ the binary (α_{binion}) and ternary (K_{ion}) recombination rate coefficient can be obtained. The example of the dependence of $\alpha_{\text{eff}\Sigma}$ on $[\text{He}]$ measured at $T=80 \text{ K}$ and $F_{D_2}=0.49$ is shown in upper panel of Figure 3. The examples of dependences of α_{effion} on $[\text{He}]$ for D_3^+ , H_2D^+ and HD_2^+ measured at $T=125 \text{ K}$ are shown in lower panel of Figure 3. The dependences $\alpha_{\text{effion}}(T, [\text{He}])$ were determined over broad range of temperatures and He densities. We need to consider several limiting factors in order to obtain reliable binary and ternary recombination rate coefficients. In

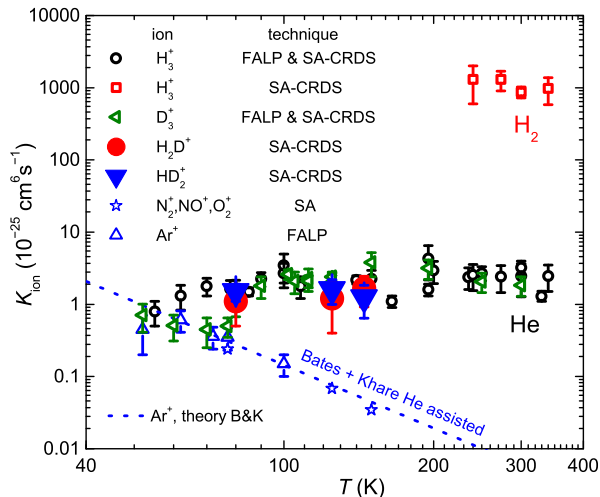


Fig. 4. Temperature dependences of the ternary recombination rate coefficients of helium assisted recombinations measured for H_3^+ [9], D_3^+ [10], H_2D^+ and HD_2^+ [15], [16] ions. The values of ternary recombination rate coefficient obtained for Ar^+ ions in helium [18] and for a mixture of atmospheric ions in helium [19] are plotted for comparison. The dashed line denotes the classical theoretical prediction by Bates and Khare [20] scaled for Ar^+ ion in helium by reduced mass. Note the substantial difference between the values of ternary recombination rate coefficients obtained for H_3^+ in helium and those measured in H_2 buffer gas [14].

plasma in $\text{He}/\text{Ar}/\text{H}_2$ or $\text{He}/\text{Ar}/\text{D}_2$ gas mixture the recombination rate coefficients for H_3^+ or D_3^+ can be measured relatively simply, because just one type of ions is present in the afterglow. In $\text{He}/\text{Ar}/\text{H}_2/\text{D}_2$ gas mixture the situation is more complicated, because at least 8 processes (rate coefficients) are influencing the plasma decay and actual $\alpha_{\text{eff}\Sigma}$ depends on T , $[\text{He}]$, $[\text{H}_2]$, $[\text{D}_2]$ and F_{D_2} .

For over ten years we have been studying electron-ion recombination of the H_3^+ cation and its deuterated isotopologues H_2D^+ , HD_2^+ and D_3^+ using flowing and stationary afterglow techniques. Essential result in these studies was the discovery that there exists a very efficient ternary neutral assisted recombination process, which is at 300 K already at few thousands pascal of He comparable with binary recombination [2,10]. Ternary recombination assisted by molecular hydrogen is by another three orders of magnitude more efficient [14]. The ternary recombination rate coefficients for H_3^+ , H_2D^+ , HD_2^+ and D_3^+ ions measured by our group so far are summarised in Figure 4 (see also Refs. [9,16]). For comparison some data for ternary recombination of Ar^+ and other ions are also included in the figure.

4 Summary and conclusion

The recombination of H_3^+ , H_2D^+ , HD_2^+ and D_3^+ ions with electrons have been recently studied at temperatures ranging from 50 K up to 340 K in He buffered afterglow plasma. In the studies the flowing afterglow (CRYO-FALP) and the stationary afterglow with CRDS

spectrometer (SA-CRDS) were used to measure effective recombination rate coefficients (α_{eff}) of mixtures of ions and their dependences on temperature, He buffer gas density ($[\text{He}] = 10^{16} - 10^{18} \text{ cm}^{-3}$) and on densities of H_2 and D_2 . From measured dependences $\alpha_{\text{eff}} = \alpha_{\text{eff}}(T, [\text{He}], [\text{H}_2], [\text{D}_2])$ over broad range of plasma parameters we were able to determine binary (α_{binH_3} , $\alpha_{\text{binH}_2\text{D}}$, α_{binHD_2} , α_{binD_3}) and ternary (K_{H_3} , $K_{\text{H}_2\text{D}}$, K_{HD_2} , K_{D_3}) recombination rate coefficients for H_3^+ , H_2D^+ , HD_2^+ and D_3^+ ions (see also Refs. [10,16]). For all four ions we observed very strong He assisted ternary recombination which is comparable with binary recombination already at He densities of $[\text{He}] = 1 \times 10^{17} \text{ cm}^{-3}$. We have studied plasma thermalisation during the afterglow in $\text{He}/\text{Ar}/\text{H}_2/\text{D}_2$ gas mixtures. The results confirm that at conditions used in present recombination studies the afterglow plasma is thermalised and the excited particles are effectively removed. Our results provide more detailed picture of recombination processes in hydrogen and deuterium containing low temperature plasmas, for instance those used in spectroscopy and in technological applications.

This work was partly supported by Czech Science Foundation projects GACR 15-15077S, GACR 17-08803S, GACR 17-18067S, and Charles University Grant Agency project GAUK 1583517.

References

1. M. Larsson, A.E. Orel, *Dissociative recombination of molecular ions* (Cambridge University Press, Cambridge, 2008)
2. J. Glosík, R. Plašil, T. Kotřík, P. Dohnal, J. Varju, M. Hejduk, I. Korolov, Š. Roučka, V. Kokouline, *Mol. Phys.* **108**, 2253 (2010)
3. B. Parise, A. Belloche, F. Du, R. Güsten, K.M. Menten, *Astron. Astrophys.* **526**, A31 (2011)
4. T.J. Millar, *Astron. Geophys.* **46**, 2.29 (2005)
5. A. Das, L. Majumdar, S.K. Chakrabarti, D. Sahu, *New Astron.* **35**, 53 (2015)
6. T. Albertsson, D.A. Semenov, A.I. Vasyunin, T. Henning, E. Herbst, *Astrophys. J., Suppl. Ser.* **207**, 27 (2013)
7. O. Sipilä, P. Caselli, J. Harju, *Astron. Astrophys.* **554**, A92 (2013)
8. P. Dohnal, M. Hejduk, P. Rubovič, J. Varju, Š. Roučka, R. Plašil, J. Glosík, *J. Chem. Phys.* **137**, 194320 (2012)
9. M. Hejduk, P. Dohnal, P. Rubovič, Á. Kálosi, R. Plašil, R. Johnsen, J. Glosík, *J. Chem. Phys.* **143**, 044303 (2015)
10. R. Johnsen, P. Rubovič, P. Dohnal, M. Hejduk, R. Plašil, J. Glosík, *J. Phys. Chem. A* **117**, 9477 (2013)
11. Á. Kálosi, P. Dohnal, L. Augustovičová, Š. Roučka, R. Plašil, J. Glosík, *Eur. Phys. J.: Appl. Phys.* **75**, 24707 (2016)
12. T. Kotřík, P. Dohnal, Š. Roučka, P. Jusko, R. Plašil, J. Glosík, R. Johnsen, *Phys. Rev. A* **83**, 032720 (2011)
13. O. Asvany, E. Hugo, F. Müller, F. Kühnemann, S. Schiller, J. Tennyson, S. Schlemmer, *J. Chem. Phys.* **127**, 154317 (2007)
14. J. Glosík, P. Dohnal, P. Rubovič, Á. Kálosi, R. Plašil, Š. Roučka, R. Johnsen, *Plasma Sources Sci. Technol.* **24**, 065017 (2015)
15. P. Dohnal, Á. Kálosi, R. Plašil, Š. Roučka, A. Kovalenko, S. Rednyk, R. Johnsen, J. Glosík, *Phys. Chem. Chem. Phys.* **18**, 23549 (2016)

16. R. Plašil, P. Dohnal, Á. Kálosi, Š. Roučka, R. Johnsen, J. Glosík, *Plasma Sources Sci. Technol.* **26**, 035006 (2017)
17. L. Pagani, C. Vastel, E. Hugo, V. Kokoouline, C.H. Greene, A. Bacmann, E. Bayet, C. Ceccarelli, R. Peng, S. Schlemmer, *Astron. Astrophys.* **494**, 623 (2009)
18. P. Dohnal, P. Rubovič, T. Kotrík, M. Hejduk, R. Plašil, R. Johnsen, J. Glosík, *Phys. Rev. A* **87**, 052716 (2013)
19. Y.S. Cao, R. Johnsen, *J. Chem. Phys.* **94**, 5443 (1991)
20. D.R. Bates, S.P. Khare, *Proc. Phys. Soc.* **85**, 231 (1965)

Cite this article as: Juraj Glosík, Petr Dohnal, Ábel Kálosi, Lucie D. Augustovičová, Dmytro Shapko, Štěpán Roučka, Radek Plašil, Electron-ion recombination in low temperature hydrogen/deuterium plasma, *Eur. Phys. J. Appl. Phys.* **80**, 30801 (2017)